Performance of Practical Receiver Schemes for Impulsive UWB Modulation on a Real MV Power Line Network

Fabio Versolatto*, Andrea M. Tonello*, Mauro Girotto*, and Carlo Tornelli†
* DIEGM - Università di Udine - Via delle Scienze 208 - 33100 Udine - Italy
e-mail: {fabio.versolatto, tonello, mauro.girotto}@uniud.it
† RSE SpA - Via Rubattino 54 - 20143 Milano - Italy
e-mail: carlo.tornelli@rse-web.it

***Abstract*—We consider the deployment of impulsive ultra wide band (I-UWB) modulation for power line communications (PLC) on medium voltage (MV) networks. We firstly describe several receiver structures, and practical channel detection algorithms based on a data-aided approach. The joint estimation of the channel response and the noise correlation is also considered. Then, we address the system performance on real MV channels. The channels have been measured in a real MV test network. Results are provided in terms of bit error rate, with a power spectral density constraint.**

I. Introduction

Power line communications exploits the existent electrical infrastructure for communication purposes. PLC is classified in narrowband and broadband PLC. Broadband PLC provides high-speed communications by exploiting the higher frequency range. Due to EMC constraints, commercial standards operate in the 2-30 MHz frequency band, and they ensure a peak data rate of 200 Mbps [1]. Communications up to 100 MHz have shown to be feasible, providing a peak data rate of about 1 Gbps [2]. According to the FCC regulations, broadband PLC can be referred to as ultra wide band (UWB) communications because the ratio between the band and the central carrier is greater than 0.2.

Multicarrier modulation is the dominant transmission technology in PLC. Commercial standards use orthogonal frequency division multiplexing schemes for both narrowband and broadband PLC. However, impulsive ultra wide band (I-UWB) modulation has shown to be an attractive alternative for both high-speed and command and control applications. I-UWB was firstly presented in wireless, where it is known as impulse radio. The impulse modulation maps the information data into short duration pulses followed by a guard time. During the guard time, the transmitter is silent in order to cope with the channel time dispersion. The optimal receiver is based on the matched filter concept [3]. To this aim, it requires the knowledge of the channel response and, in the presence of colored noise, the noise correlation. This is the case for instance of PLC. Practical frequency domain receiver algorithms for high-speed multiuser in-home PLC were presented in [4]. Neglecting the noise correlation, a simpler though sub-optimal implementation of the receiver is possible. In this respect, a practical time-domain implementation of the receiver was described in [5]. Later, a simplified synchronization and channel estimation algorithm was proposed in [6] for the sub-optimal PLC receiver.

In this paper, we focus on the communications over MV lines. Medium voltage PLC plays an important role in the emerging Smart Grid, i.e., the decentralized management of the energy distribution network [7]. In this respect, we have investigated the performance of I-UWB modulation on real MV channels. We have firstly performed a measurement campaign in the MV network that feeds the industrial complex where the RSE laboratories are located. Then, in [8], we have described the statistics of the MV channels and we have shown the performance of I-UWB for the optimal and the sub-optimal receiver, assuming the ideal implementation of the receiver structures and the perfect knowledge at the receiver side of both the channel response and the noise correlation. We have found that I-UWB modulation is suitable for low data rate command and control applications on MV channels. Furthermore, we have provided the optimal value of the transmission bandwidth and the guard interval.

In this paper, we investigate the performance of practical receiver algorithms. We limit the analysis to three channels extracted from the measured data set presented in [8]. The three channels are representative of the worst, average and the best case. We firstly study the performance of the practical receiver algorithms assuming perfect synchronization and channel estimation. We compare the results to the ideal ones. Then, we address the performance in the presence of practical channel estimation and synchronization. Furthermore, the joint channel and noise estimation is also addressed.

The remainder of this paper is organized as follows. In

This work has been partly funded by the Research Fund for the Italian Electrical System under the Contract Agreement between RSE (formerly known as ERSE) and the Ministry of Economic Development - General Directorate for Nuclear Energy, Renewable Energy and Energy Efficiency stipulated on July 29, 2009 in compliance with the Decree of March 19, 2009.

Section II, we discuss the application scenario. In Section III and IV, we describe the receiver structures and the detection algorithms, respectively. In Section V, we show the numerical results that allow for evaluating the performance of different schemes. Finally, some conclusions follow.

II. Description of the Application Scenario

We performed an exhaustive measurement campaign on a real-life MV network and we obtained a set of MV measured channel responses. In this section, we firstly describe the acquisition process and the three representative channels that have been selected for the best, average and worst case. Then, we describe the noise model.

A. Medium Voltage PLC Channel

We consider the MV network that feeds the industrial complex where the RSE laboratories are located. In [8], we described the network and the acquisition setup. Basically, we injected a wideband pulse from the transmitter coupler and we acquired the signal received by all the other couplers. The acquisitions have been performed in the time domain. We collected the channel responses of 42 links and the measures have validity up to $B = 55\,MHz$. In detail, we obtained the channel frequency response by means of discrete Fourier transform (DFT), with a frequency step size of $10\,kHz$. Furthermore, we window the channel impulse response to include $95\,\%$ of the channel energy.

In [8], we have studied the statistics of the channel data set. Herein, we consider only three channels, that are representative of the worst, average and best case. We select the channels as follows. For every frequency f, we pick the 10-th, the 50-th and the 90-th percentile of the measured frequency responses, and we obtain the worst, the average and the best target functions, i.e., $H^{10}(f)$, $H^{50}(f)$ and $H^{90}(f)$, respectively. We point out that the target functions are not measured channels. Therefore, we select the three measured channels whose frequency response is close to the target functions. We proceed as follows. We define the metric

$$\Gamma^n(l) = \int_0^B \left(\log|H_l(f)| - \log|\hat{H}^n(f)|\right)^2 df, \qquad (1)$$

where $n \in \{10, 50, 90\}$, and $l = 1, \ldots, 42$ denotes the l-th measured channel. Then, we search for the channel which minimizes the metric in (1), namely, $H^n(f) = H_{m_n}(f)$, where

$$m_n = \underset{l=1,\ldots,42}{\operatorname{argmin}} \{\Gamma^n(l)\}. \qquad (2)$$

For $n = 10$, 50, 90, $H^n(f)$ is the measured channel that is representative of the worst, average and best case, respectively. In Fig. 1, we show the amplitude and the phase of the frequency response of the three channel instances.

B. Background Noise Model

Although the noise in PLC is due to several sources, it can be modelled as the sum of two contributions, i.e., the background and the impulse noise. The first is stationary, and it is modelled as additive colored Gaussian noise. In this work, we focus on the background noise. We model the noise power spectral density (PSD) as follows [9]

$$N(f) = 37 \cdot e^{-0.17f/10^6} - 105 \quad [dBm/Hz]. \qquad (3)$$

We assume the model to be valid up to 55 MHz.

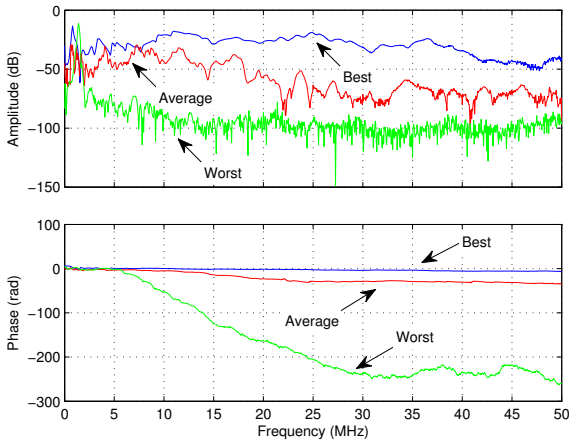

Fig. 1. Frequency response in amplitude and phase of the representative channels for the best, average and worst case scenario.

III. I-UWB System Model

In I-UWB, information symbols are mapped into short duration pulses followed by a guard time. In Fig. 2, we show the transmission scheme. We denote with T_f the frame period and we assume the symbols to be transmitted with a rate $1/T_f$. Therefore, the transmitted signal can be written as

$$x(t) = \sum_k b_k g_{tx}(t - kT_f), \qquad (4)$$

where b_k is the information symbol of the k-th frame, and $g_{tx}(t)$ is the transmission pulse, namely, the monocycle. We focus on binary I-UWB, and thus we assume the symbols to belong to the alphabet $\{-1, 1\}$. Furthermore, we shape the monocycle in order to avoid the transmission in the frequency range where the PSD of the background noise is high, i.e., in the lower frequency range. We choose the second derivative of the Gaussian pulse, which reads

$$g_{tx}(t) = \left(1 - \pi\left((t - D/2)/T_0\right)^2\right) e^{-\frac{\pi}{2}((t-D/2)/T_0)^2}, \qquad (5)$$

where $D = 6T_0$ is the pulse duration, and T_0 accounts for the transmission bandwidth. In detail, we define the transmission bandwidth B as the lowest frequency beyond which the average PSD of the transmitted signal falls below 30 dB of its maximum value P.

At the receiver side, we filter the received signal $y(t)$ with an analog front-end filter to obtain

$$u(t) = \sum_k b_k g_{tx} * g_{ch} * g_{fe}(t - kT_f) + d(t), \qquad (6)$$

where $g_{ch}(t)$, $g_{fe}(t)$ and $d(t) = n * g_{fe}(t)$ are the channel impulse response, the front-end filter impulse response and the

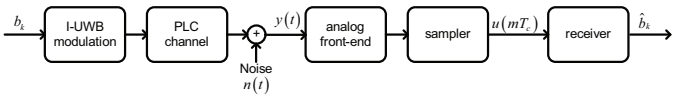

Fig. 2. Transmission scheme of an I-UWB system

filtered background colored noise, respectively. Furthermore, we refer to the equivalent channel response as $g_{eq}(t) = g_{tx} * g_{ch} * g_{fe}(t)$, and we match the front-end filter to the transmitter monocycle, i.e., $g_{fe}(t) = g_{tx}(-t)$.

We consider a packet transmission where the packets are composed of a training bit sequence followed by 100 bits of information. In the following, we describe the practical implementation of several receivers based on the matched filter concept. In all cases, we assume discrete-time processing, i.e., we sample the output of the front-end filter with period $T_c = T_f/M$, where M denotes the number of samples/frame.

A. Matched Filter Receiver

The matched filter receiver neglects the correlation of the noise, and thus it is matched only to the waveform given by the convolution of the monocycle and the channel impulse response [3]. Basically, it is optimal in the presence of additive white Gaussian noise and no inter symbol interference (ISI). We implement the matched filter receiver as follows. Since the analog front-end is matched to the monocycle, i.e., $g_{fe}(t) = g_{tx}(-t)$, we filter $u(mT_c)$ with the matched filter $g_{rx}(mT_c) = g_{ch}^{-}(mT_c) = g_{ch}(-mT_c)$ to obtain the following metric

$$\Lambda(k) = \sum_m u(mT_c) g_{rx}(kT_f - mT_c). \tag{7}$$

Then, we make a threshold decision on the metric in (7). Strictly, the detected symbol in the k-th frame is given by

$$\hat{b}(kT_f) = \text{sign}\left\{\Lambda(k)\right\}. \tag{8}$$

We refer to this receiver as matched filter (MF) receiver.

B. Equivalent-Matched Filter Receiver

In PLC the background noise is colored, and thus the MF receiver is not optimal. To improve the performances of the MF implementation, we propose to match the receiver to the equivalent filter $g_{eq}(t)$ instead of $g_{ch}(t)$. In detail, we filter $u(mT_c)$ with the matched filter $g_{rx}(mT_c) = g_{eq}(-mT_c)$, and we obtain the decision metric in (7). Then, we decide for the symbol transmitted in the k-th frame according to (8). We refer to this implementation as equivalent-matched filter (E-MF) receiver. Basically, the frequency response of the monocycle approximates the shape of the inverse of the noise PSD in the lower frequency range. Since the front-end filter is matched to the monocycle, it acts as a whitening filter in the lower frequency range, where we experience the highest levels of disturbance. Hence, the E-MF is expected to perform better than the simple MF receiver, as it will be shown in the numerical results. Furthermore, we point out that the estimation of the equivalent channel impulse response is simple (see Section IV-A).

C. Noise-Matched Filter Receiver

The optimal receiver in the presence of colored noise requires the perfect knowledge of the noise correlation [3]. According to the notation of Fig. 2, we firstly define the correlation function of the sampled noise as $R_n(mT_c) = E\left[n(mT_c + lT_c)n(lT_c)\right]$, where $E[\cdot]$ is the expectation operator, and we denote with $R^{-1}(mT_c)$ the convolutional inverse of $R_n(mT_c)$, i.e., $R_n^{-1} * R_n(mT_c) = \delta(mT_c)$.

Then, we filter the output of the analog front-end with the matched filter $g_{rx}(mT_c) = R_n^{-1} * g_{ch}^{-}(mT_c)$. We obtain the metric in (7). Finally, we decide for the transmitted symbol according to (8). We refer to this receiver structure as noise-matched filter (N-MF) receiver.

D. Frequency Domain Implementation of the N-MF Receiver

We derive the frequency domain implementation of the noise-matched filter receiver. We follow the approach described in [4]. We focus on the output of the sampler, namely, $u(mT_c)$, and we introduce the vector notation $\mathbf{u} = [u(0),\ u(T_c),\ u(2T_c),\ \ldots]^T$, where $\{\cdot\}^T$ indicates the transposition. We partition the vector into blocks of length $M = T_f/T_c$, i.e.,

$$\mathbf{u}_k = \left[u(kMT_c),\ \ldots,\ u((M-1+kM)T_c)\right]^T.$$

Basically, the k-th block vector contains the samples of the k-th received frame. Further, we denote with $\mathbf{d}_k$ the vector of the noise samples of the k-th frame. Now, if we neglect the noise correlation among frames and we do not experience ISI, we can process each frame independently. Therefore, we compute the M-point discrete Fourier transform (DFT) of the k-th frame and we obtain

$$\mathbf{U}_k = b_k \mathbf{G}_{eq} + \mathbf{D}_k \tag{9}$$

where b_k is the symbol transmitted in the k-th frame, and $\mathbf{U}_k$, $\mathbf{D}_k$ and $\mathbf{G}_{eq}$ are $M \times 1$ vectors of the M-point DFT of $\mathbf{u}_k$, $\mathbf{d}_k$ and the equivalent impulse response vector $\mathbf{g}_{eq} = [g_{eq}(0),\ \ldots,\ g_{eq}(M-1)]$, respectively. The M-point DFTs are computed at the frequencies $f_n = n/MT_c$, $n = 0,\ \ldots,\ M-1$. Now, we express the likelihood function in the frequency domain from (9), we maximize it and we obtain the following decision metric [4]

$$\Lambda(k) = b_k\ \mathbf{G}_{eq}^H \mathbf{R_D}^{-1} \mathbf{U}_k, \tag{10}$$

where $\{\cdot\}^H$ indicates the hermitian transpose, and $\mathbf{R_D}$ is the noise correlation in a frame, i.e., $\mathbf{R_D} = \mathbf{R_{D_k}} = E\left[\mathbf{D}_k \mathbf{D}_k^H\right]$ $\forall\ k$. Note that $\mathbf{R_D}$ is constant for each frame because we assume the noise to be stationary. We compute it as described in Section IV-B for the MMSE algorithm. Finally, the decision on the k-th transmitted symbol is accomplished looking at sign of (10), i.e., according to (8). We refer to this receiver structure as frequency domain (FD) receiver.

IV. Practical Detection Algorithms

We follow a data-aided approach. Basically, we exploit the training bit sequence to detect and estimate the channel. We assume the training bit sequence to be long N_t bits and to be known at the receiver side.

A. Time Domain Detection Algorithms

The E-MF receiver requires the knowledge of the equivalent filter response and the synchronization istant. We follow the approach presented in [5]. Basically, we synthesize the equivalent channel impulse response as the composition of N_p multipath components that reads

$$g_{eq}(mT_c) = \sum_{p=0}^{N_p-1} \alpha_p \delta((m-p)T_c - \Delta), \qquad (11)$$

where α_p is the value of the equivalent channel response at the instant $pT_c + \Delta$. Now, we search for the delay Δ and the amplitudes α_p. For each sample $u(mT_c)$, we compute the metric

$$\chi(mT_c) = \sum_{k=0}^{N_t-1} b_k u(mT_c + kT_f), \qquad (12)$$

where b_k is the k-th bit of the training sequence. Then, we find

$$m = \underset{l\in\mathbb{Z}}{\operatorname{argmax}} \left\{ \sum_{i=0}^{N_p-1} \left|\chi(lT_c + iT_c)\right|^2 \right\} \qquad (13)$$

and we obtain the delay $\Delta = mT_c$. Finally, the equivalent channel amplitude coefficients are given by $\alpha_p = \chi(\tau_p) / (N_t E_{tx})$, where $\tau_p = pT_c + \Delta$ and E_{tx} is the energy of the monocycle. In the following, we assume $N_p = M$.

B. Frequency Domain Channel Detection Algorithms

Now, we focus on the channel estimation problem in the frequency domain. We study two channel estimation algorithms, i.e., the linear minimum mean square error (MMSE) and the recursive least square (RLS) algorithm. We firstly consider the MMSE algorithm. We follow the approach presented in [10]. We define the frame correlation matrix of the k-th received frame as $\mathbf{R}_k = \mathbf{U}_k \mathbf{U}_k^H$. Then, we estimate the correlation matrix of the noise $\mathbf{R_D}$ and the received signal $\mathbf{R_U}$ as the average of the frame correlation matrices of the N_e empty frames that precede the training sequence and the average of the frame correlation matrices of the N_t training sequence frames, respectively. Finally, we estimate the M-point DFT of the channel as

$$\hat{\mathbf{G}}_{ch} = \frac{1}{N_t} \sum_{k=0}^{N_t-1} b_k \mathbf{Q} \mathbf{W}^H \mathbf{U}_k, \qquad (14)$$

where

$$\mathbf{Q} = \mathbf{W}^{-1} \left(\mathbf{I} - \mathbf{R_D} \mathbf{R_U}^{-1}\right) (\mathbf{W}^H)^{-1}, \qquad (15)$$

$\mathbf{I}$ is the $M \times M$ identity matrix, $\mathbf{W} = diag\{\mathbf{G}_{tx}\} diag\{\mathbf{G}_{fe}\}$, and $\mathbf{G}_{tx}$ and $\mathbf{G}_{fe}$ are the $M \times 1$ vectors of the M-points DFT of the transmitted monocycle and the front-end impulse response, respectively.

Now, we focus on the RLS algorithm. The estimation of $G_{ch}(f_n)$ is independent for each frequency f_n and it is accomplished via a one-tap RLS algorithm [11] that uses the following error signal

$$e_k(f_n) = U_k(f_n) - b_k W(f_n) G_{ch,k-1}(f_n), \qquad (16)$$

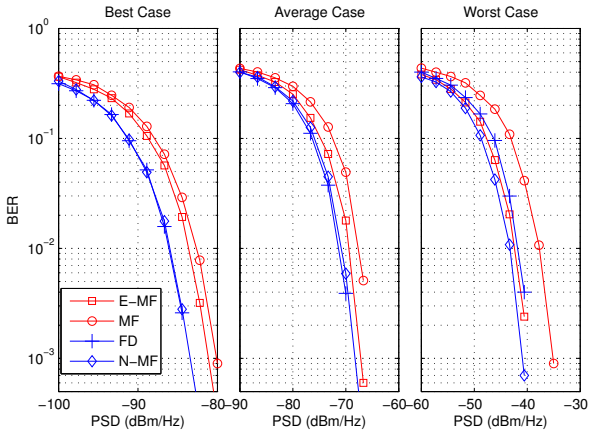

Fig. 3. Performance in BER of the receiver schemes.

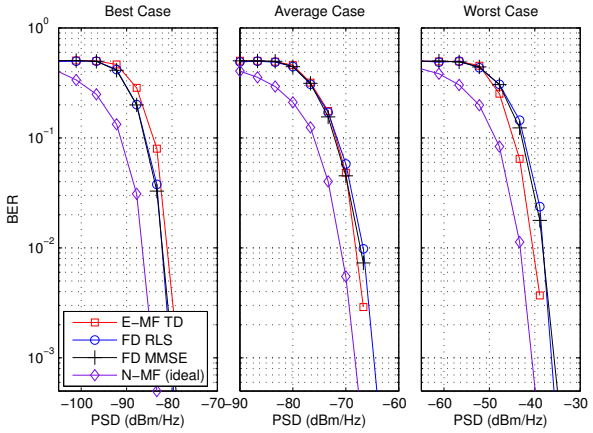

Fig. 4. Performance in BER of the practical detection algorithms. The ideal case is also reported.

where b_k, is the transmitted symbol at the k-th frame of the training sequence, and $G_{ch,k-1}(f_n)$ is the estimated channel frequency response at frequency f_n and iteration $k-1$. We refer to [12] for all the parameters of the algorithm.

In both algorithms, we limit the channel estimation to the frequency bins where the signal energy is mainly concentrated. This improves the stability. Further, we use the two-step synchronization algorithm that we have firstly presented in [12].

V. Numerical Results

In [5], we have found the values of the transmission bandwidth and the frame duration that ensure the best performance for a I-UWB transmission in the MV test network. Herein, we exploit these results, and thus we assume a transmission bandwidth $B = 20\,MHz$, and a frame duration $T_f = 5\,\mu s$. Therefore, the bit rate is fixed to 200 kbps. Further, we set $1/T_c = 50$ MHz. We present the results in terms of bit error rate, with a PSD constraint. We firstly address the performance of the receivers described in Section III. To this end, we assume perfect knowledge of the channel impulse response,

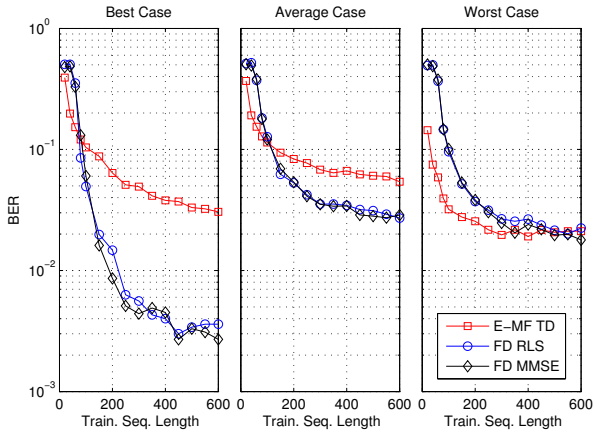

Fig. 5. Performance in BER of the practical detection algorithms as a function of the length of the training sequence.

the synchronization instant and the noise correlation function at the receiver side. In Fig. 3, we provide the results. As expected, the N-MF receiver shows the best performance in all the three cases. Furthermore, we have found that the FD receiver attains the optimal performance in the best and the average case. A slightly worsen behaviour have been found for the worst channel. This is due to the presence of ISI. In fact, a frame period of $5\,\mu s$ is not sufficiently long to cope with the time dispersion of the worst channel. Interestingly, we have also found that the E-MF outperforms the MF receiver. Hence, matching the receiver to the output of the analog front-end has shown to be beneficial. We point out that this result is not valid in general. Rather, it depends on the noise model and the shape of the monocycle.

Now, we introduce the practical channel and noise estimation. We address the performance of the E-MF receiver in combination with the time-domain estimation algorithm of Section IV-A, and the performance of the FD receiver in combination with both the RLS and the MMSE channel estimation algorithms. We refer to these schemes as E-MF TD, FD RLS and FD MMSE, respectively. We set $N_t = 100$ bits. In Fig. 4, we show the results. We have found that the practical channel and noise estimation introduces a performance loss that is approximately 8 dB for the FD receiver and between 5 and 10 dB for the E-MF TD receiver. Furthermore, we turned out the same performance for the FD RLS and the FD MMSE algorithms.

A. Influence of the Training Sequence Length

Herein, we focus on the effect of the training sequence length on the performance of practical receivers. We fix the power spectral density of the transmitted signal, and we vary N_t. We use $P = -84$ dBm/Hz, -72 dBm/Hz and -42 dBm/Hz for the best, average and worst channels, respectively. We evaluate the bit error rate of the E-MF TD, FD RLS and FD MMSE receivers. In Fig. 5, we show the results. Frequency domain channel estimation algorithms show, in general, a fast convergence. Furthermore, the RLS and the MMSE algorithms exhibits approximately the same performance.

VI. Conclusions

We have investigated the performance of practical receiver algorithms for impulsive ultra wide band modulation on a real MV test network. We have firstly compared the performance of several receivers, assuming perfect knowledge of the channel impulse response and the noise correlation at the receiver. Then, we have introduced the practical estimation algorithms for the channel response and the noise correlation. The results show that I-UWB modulation is suitable for low data rate applications over MV channels. The main strength is given by the low system complexity. In detail, we have found that the simple equivalent-match filter receiver provides low bit error rates even for values of transmitted PSD that are low, w.r.t. the typical ones of PLC. More robust transmissions can be obtained by increasing the complexity of the receiver, e.g., with the frequency domain receiver that takes into account for the noise correlation.

References

[1] Home Plug Alliance. [Online]. Available: www.homeplug.org
[2] A. M. Tonello, P. Siohan, A. Zeddam, and X. Mongaboure, "Challenges for 1 Gbps Power Line Communications in Home Networks," in *Proc. of IEEE Personal Indoor Mobile Radio Communications Symposium (PIMRC)*, September 2008, pp. 1–6.
[3] A. M. Tonello, R. Rinaldo, and L. Scarel, "Detection Algorithms for Wide Band Impulse Modulation Based Systems over Power Line Channels," in *Proc. IEEE Int. Symp. Power Line Commun. and Its App. (ISPLC)*, Apr. 2004, pp. 367–372.
[4] A. M. Tonello, "Wideband Impulse Modulation and Receiver Algorithms for Multiuser Power Line Communications," *EURASIP Journal on Advances in Signal Processing*, vol. 2007, pp. 1–14.
[5] A. M. Tonello, R. Rinaldo, and M. Bellin, "Synchronization and Channel Estimation for Wide Band Impulse Modulation over Power Line Channels," in *Proc. of Int. Symp. on Power Line Commun. and Its App. (ISPLC)*, March 2004, pp. 206–210.
[6] A. M. Tonello and N. Palermo, "Soft Detection with Synchronization and Channel Estimation from Hard Quantized Inputs in Impulsive UWB Power Line Communications," in *Proc. IEEE Int. Conf. on Ultra-Wideband (ICUWB)*, Sep. 2009, pp. 560–564.
[7] S. Galli, A. Scaglione, and Z. Wang, "For the Grid and Through the Grid: The Role of Power Line Communications in the Smart Grid," *Proc. IEEE*, vol. 99, no. 6, pp. 998–1027, May 2011.
[8] A. M. Tonello, F. Versolatto, and C. Tornelli, "Analysis of Impulsive UWB Modulation on a Real MV Test Network," in *Proc. of Int. Symp. on Power Line Commun. and Its App. (ISPLC)*, April 2011, pp. 18–23.
[9] M. Babic et al., "OPERA Deliverable D5. Pathloss as a Function of Frequency, Distance and Network Topology for Various LV and MV European Powerline Networks," 2005.
[10] J.-J. Van de Beek, O. Edfors, M. Sandell, S. K. Wilson, and P. O. Borjesson, "On Channel Estimation in OFDM Systems," in *Proc. IEEE Veh. Technol. Conf. (VTC)*, vol. 2, Jul. 1995, p. 815.
[11] Y. Kojima, H. Tomeba, K. Takeda, and F. Adachi, "RLS Channel Estimation with Adaptive Forgetting Factor for DS-CDMA Frequency-Domain Equalization," *IEICE Trans. on Commun.*, vol. E92-B, no. 5, pp. 1457–1465, May 2009.
[12] A. M. Tonello and R. Rinaldo, "A Time-Frequency Domain Approach to Synchronization, Channel Estimation, and Detection for DS-CDMA Impulse-Radio Systems," *IEEE Trans. on Wireless Commun.*, vol. 4, no. 6, pp. 3005–3017, Nov. 2005.